CORROSION PROPERTIES OF IRON AND IRON-MANGANESE SINTERED MATERIALS

M. Kupková, M. Hrubovčáková, R. Oriňáková, A. Morovská Turoňová, A. Zeleňák

Abstract

The aim of the presented study was to investigate the electrochemical corrosion behaviour of iron and iron-manganese sintered structures in a medium simulating a human body fluid environment.

Iron samples and alloys with Mn content of 30 wt.% were prepared. Their microstructure as well as degradation behaviour in Saline solution were investigated by the use of potentiodynamic tests, optical microscopy, scanning electron microscopy and energy-dispersive X-ray spectroscopy. The corrosion rates of microheterogeneous Fe-Mn alloys were found to be higher than those for a pure iron, and also higher than rates reported for homogeneous Fe-Mn alloys.

Keywords: powder metallurgy, iron, manganese, corrosion behaviour

INTRODUCTION

Because of their excellent mechanical properties, metals have been used to fabricate devices which treat, augment or replace tissues, organs, or functions of the human body for more than a century. During these years, a paradigm has been established that metals used as biomaterials should be highly corrosion-resistant to survive the physiological environment.

But in recent decades, a quite general agreement has emerged that, for certain medical applications, the corrodibility can be a desirable material's property [1]. This relates, for example, to corronary stents. There is evidence that the mechanical scaffolding effect provided by a stent is needed only temporarily for a period of 3-6 (6-12) months after stent implantation, during which arterial remodelling and healing occur. After this period, the presence of stent within a body cannot provide any beneficial effect. Contrarily, the permanent implant in the arterial wall can trigger later complications such as restenosis, thrombosis, etc. So, the temporary stent that can biodegrade in situ in a controlled, harmless way, forming non-toxic degradation products which are readily excreted, would be clearly preferable over the currently-used permanent stents.

With respect to the above-mentioned, the iron based alloys which consist of trace elements existing in the human body are promising candidates for temporary stent materials.

Stents made of pure iron were implanted into various mammals [2], [3] and [4]. The results showed no signs of iron overload or iron-related organ toxicity, there was no evidence for local toxicity due to corrosion products. However, iron stents remained mainly intact for up to a year after implantation. In addition, the mechanical properties of pure iron are modest and not particularly well suited for use as stents. To accelerate degradation and

Miriam Kupková, Monika Hrubovčáková, Adam Zeleňák, Institute of Materials Research, Slovak Academy of Sciences, Košice, Slovak Republic

Renáta Oriňáková, Andrea Morovská Turoňová, Department of Physical Chemistry, Institute of Chemistry, Faculty of Science, P.J. Šafárik University, Košice, Slovak Republic

improve mechanical properties, Hermawan et al. [5-7] studied Fe–Mn alloys. From a biological point of view, the excess of manganese is not reported to be toxic in the cardiovascular system [7]. Moreover, considering the very light weight of a stent, which is 50–100 mg depending on design, the release of elements from the corroding alloy could be expected to be lower than their toxic level in the blood.

Fe–Mn alloys, containing between 20 and 35 wt.% manganese, were compacted and sintered from elemental Fe and Mn powders. After several rolling-sintering cycles, the samples exhibited mechanical properties comparable to those of the SS316L alloy [5,6] as they possessed a similar austenite (γ) structure. The corrosion rates of samples in a modified Hank's solution were determined by the use of an immersion method. The corrosion rate of the material Fe-25 wt.% Mn was found to be 0.52 mm year^{-1}, which is slightly higher than the rate 0.44 mm year^{-1} found for Fe-35 wt.% Mn. This could be related to the bi-phase structure of Fe-25 wt.% Mn sample, where ε-martensite and γ-austenite phases coexist and serve as micro-galvanic sites accelerating corrosion. The Fe-35 wt.% Mn has only γ-austenite phase. The degradation rates of both materials were higher than those of pure iron (0.22-0.24 mm year^{-1}) [7].

Nevertheless, degradation rates of Fe-Mn alloys may still be considered too low for practical applications. In that context, new biodegradable alloys were developed by adding other elements, e.g. Fe–Mn–Pd [8], Fe-Mn-C-Pd [9].

In the above-mentioned binary Fe-Mn systems, the iron and manganese were uniformly distributed in the material. In this contribution we present the results of an attempt to accelerate the degradation of Fe-Mn systems by creation of microgradients in concentration of elements in an alloy. Due to this variation in chemical composition on small scales, each grain can be considered as composed of „different metals" in mutual contact, which after immersion into electrolyte could result in the presence of many additional micro-galvanic cells initiating and accelerating corrosion in comparison with homogeneous sample.

EXPERIMENTAL

Fe-30 wt.% Mn alloys were prepared from elemental powders of iron (water-atomized iron powder, Höganäs, ASC 100.29 grade) and manganese (fraction < 45 μm). The powders were mixed in a turbula mixer for 20 minutes. The powder mixtures were cold pressed in a cylindrical die at 600 MPa (ϕ10x10 mm^3). No lubricant was added to the powder, nor were the die walls lubricated.

The specimens were isothermally sintered in a laboratory tube furnace ANETA at the temperature of 1120ºC for 60 min and cooled to room temperature. The heating and cooling rate was kept at 10°C/min. The gas mixture of 10% H_2 – 90% N_2 (purity of 5.0) was used as a sintering atmosphere. The flow-rate of the processing atmosphere was 4 l/min. Atmosphere drying was performed utilizing zeolite molecular sieve dryers. The inlet dew point (monitored by the SHAW Super-Dew Hygrolog was ~ -59°C. Compact density values before and after sintering were obtained by weighing and measuring the dimensions of compacts.

Metallographic specimens were polished with 0.1μm diamond paste and etched in 2% nital solution. The microstructure of specimens was investigated using an optical microscope (OLYMPUS GX71, Japan) and scanning electron microscope coupled with the energy dispersive spectrometer (JEOL JSM-7000F, Japan with EDX INCA).

Corrosion properties were investigated using potentiodynamic polarization method by using the Autolab Potentiostat PGSTAT 302N. Measurements were carried out with a conventional three-electrode arrangement with the Ag/AgCl reference electrode,

platinum counter electrode and iron or iron-manganese sample as the working electrode. The potentiodynamic polarisation experiments were performed in an electrolyte Saline (9 g/l NaCl solution, pH 7.2). In all experiments, the temperature was maintained at 37°C ± 1°C. Polarisation curves were obtained by varying the applied potential from -1100 mV up to -200 mV at a scan rate of 12.5 mV/s. The corrosion current, corrosion potential and corrosion rate were determined by the use of the Tafel extrapolation method.

MICROSTRUCTURE

Figure 1 shows a microstructure of samples sintered at the temperature 1120°C. In Figure 1b, the differences in Mn concentration are made visible by etching. The iron-rich cores of original iron powder particles are less affected by etching (bright) and the regions around, consisting of the Fe-Mn solid solution, are attacked by the etching reagent (dark). It is also possible to find "free" manganese in pores and on boundaries of original iron particles.

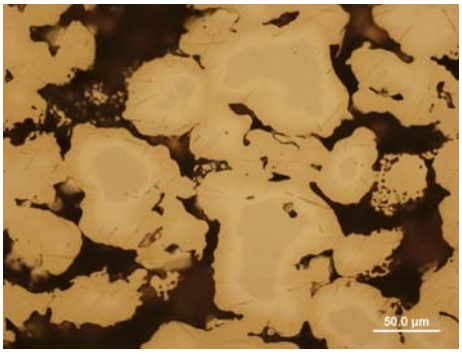

Fig.1a. Structure of sample Fe-30 wt.% Mn sintered at 1120°C.

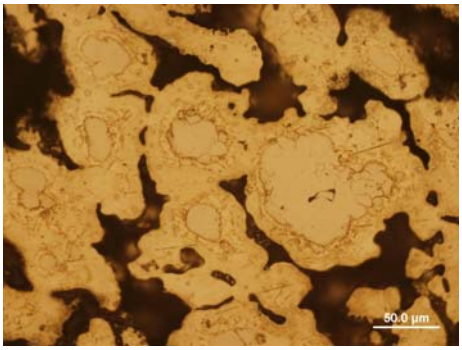

Fig.1b. Structure of sample Fe-30 wt.% Mn sintered at 1120°C, nital etched.

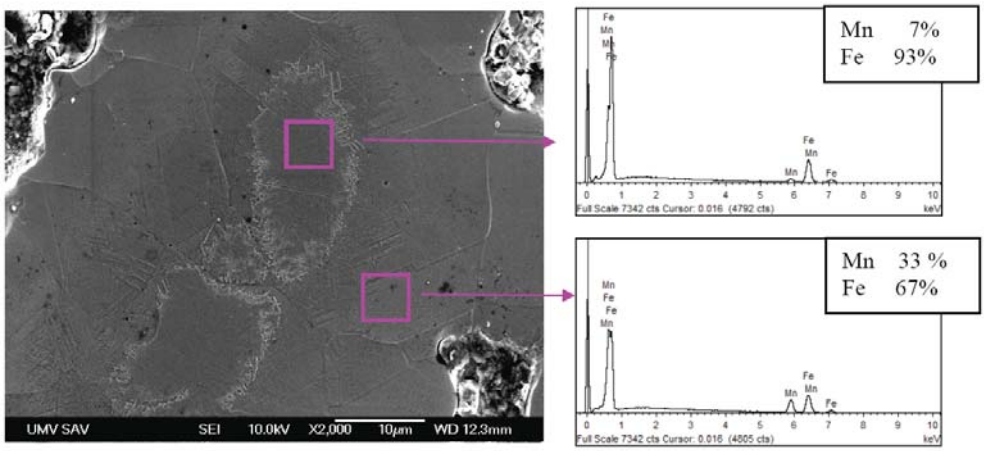

Fig.2. SEM and EDX analysis of sintered sample Fe-30 wt.% Mn after sintering at 1120°C for 60 min; a) centre of iron grain (particle), b) area near the surface of the iron grain (particle).

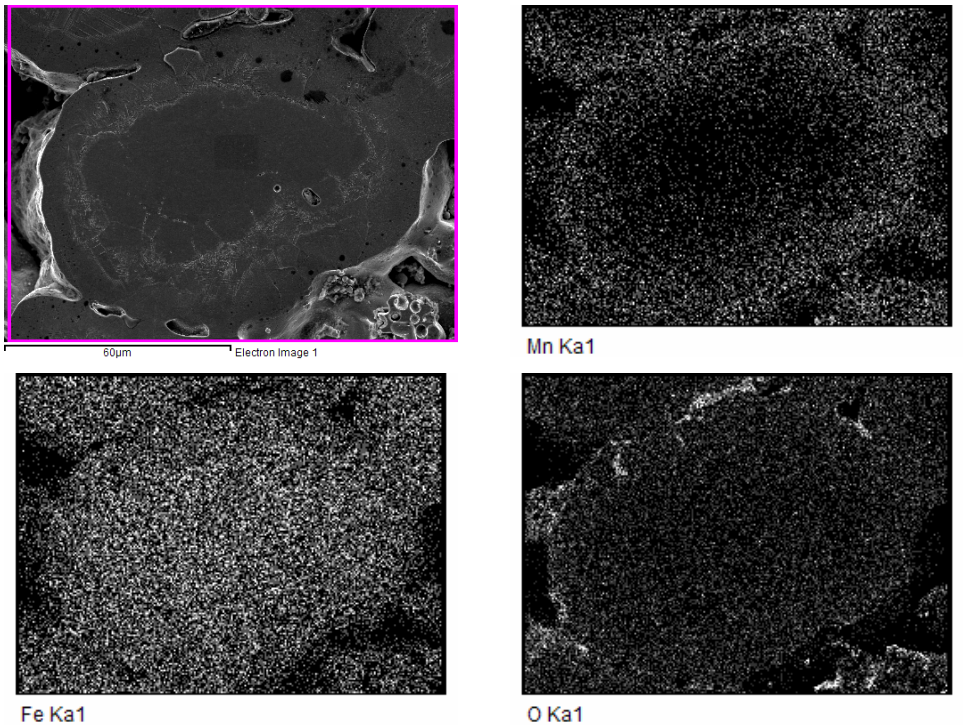

Fig.3. SEM and EDX analysis of sintered Fe-30 wt.% Mn sample.

In Figures 2 and 3, the results of EDX analysis of a particle of sintered sample Fe-30 wt.% Mn are presented. The results show that the manganese partly diffused to iron matrix, so there is an increased amount of manganese on the surface of the iron particle. The analysis also revealed the presence of oxygen, Fig.3. This should be a consequence of a high affinity of manganese to oxygen, implying the possibility of considerable oxidation during sample processing. Fe-Mn materials are exposed to considerable oxidation during heating stage even when a high purity sintering atmosphere is applied [10].

CORROSION OF SINTERED SAMPLES

Electrochemical degradation of prepared iron and iron-manganese materials in 37°C Saline solution (9 g/l NaCl solution, pH 7.2) was examined by means of polarisation curves.

Polarisation curves were obtained by varying the applied potential from -1100 mV up to -200 mV at the scan rate of 12.5 mV/s. Five cycles of potentiodynamic polarisation were registered for Fe and Fe-Mn samples. The polarisation curves are shown in Fig.4.

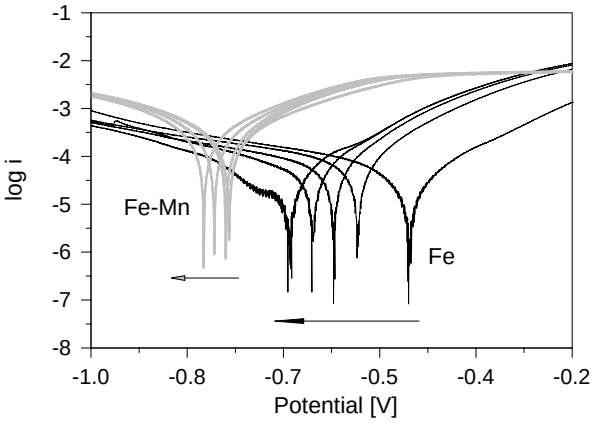

Fig.4. Polarisation curves for iron and iron manganese samples in saline solution at 37°C; semilogarithmic form.

The corrosion potential moved towards negative values before stabilization. This negative shift gives an indication about the increased corrosion susceptibility of iron and iron-manganese samples. Generally, it was found that the corrosion resistivity decreases with an increasing number of cycles. The air-formed primary oxide film, which to some extent protected the material, was dissolved during the first cycle of polarisation thereupon in next cycles the samples showed a higher tendency to corrode. Fe-Mn alloy has more negative corrosion potential than the pure iron has, which indicates worse corrosion resistance.

The degradation rate was determined from potentiodynamic polarization curves.

It is assumed that uniform corrosion is occurring and the process of oxidation does not occur selectively for any component of the alloy. Then the corrosion rate (R_M) is given as

$$R_M = \frac{i_{corr}}{\rho F \sum_i \frac{n_i c_i}{M_i}}.$$

Here i_{corr} is the corrosion current density, ρ is the alloy mass density, c_i is the mass fraction of the ith component of the alloy, M_i is the molar mass of the ith component and n_i is the number of electrons lost when oxidizing the ith component atom under conditions of the corrosion process (the valence of the ith component element).

When non-uniform corrosion processes are occurring, the above relation underestimates the true value of the corrosion rate.

All values of corrosion potential (E_{corr}) for five cycles, the estimated corrosion current densities (i_{corr}) and corrosion rates are summarised in Table 1. The corrosion rates of iron-manganese compacts are higher than those of iron compacts. The higher susceptibility of Fe-Mn alloys to corrosion could be ascribed to the presence of Fe-Mn solid solution, to the gradients in concentrations of the alloy's elements, and to the presence of pores and grain boundaries.

Tab.1. The obtained values of E_{corr}, i_{corr} and corrosion rates for Fe, Fe-30Mn specimens.

Sample	E_{corr} [mV]					i_{corr} [A/m^2]	Corrosion rate [mm/year]
	1. cycle	2. cycle	3. cycle	4. cycle	5. cycle	5. cycle	5.cycle
Fe	-495.1	-556.2	-596.1	-633.2	-680.0	0.12	0.16
Fe30Mn	-770.8	-770.3	-775.9	-795.1	-812.6	1.14	1.98

In Figures 5 and 6, the images of iron and iron-manganese samples after the corrosion test and details of corroded surfaces are shown.

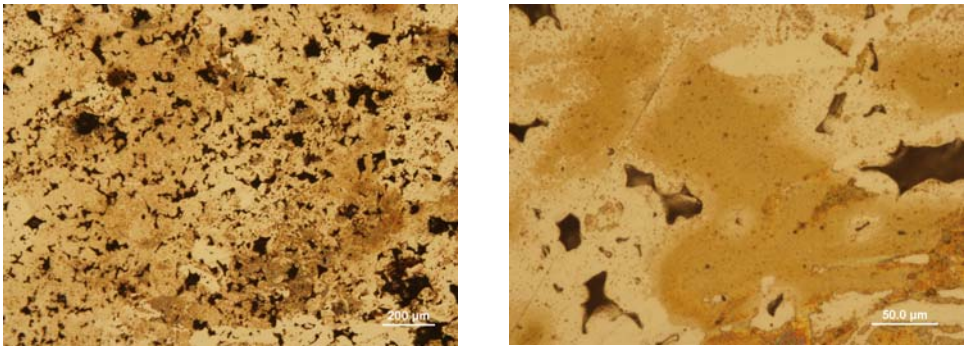

Fig.5. Corroded surface of sintered iron cylinder.

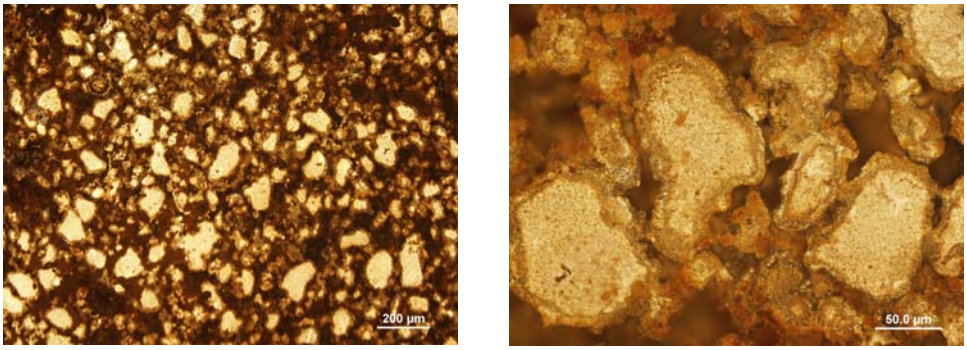

Fig.6. Corroded surface of sintered Fe-30 wt. % Mn sample.

For the iron samples, uniform corrosion spread out over the entire iron surface was observed. Sintered specimens prepared from Fe-30 wt.% Mn show an increased corrosion attack near the boundaries of iron particles, which is on areas with an increased amount of manganese (Fig.6).

CONCLUSION

Fe and Fe-Mn materials were prepared by the powder metallurgical route. Namely, Fe and mixed Fe-Mn powders were pressed into cylindrical samples and sintered at 1120^{o}C.

The microstructure of obtained materials was analyzed and their corrosion potential and corrosion rates in saline solution at 37°C were investigated.

The degradation rate of a sample from pure iron is about 0.16 mm year^{-1}. Alloying of Fe with Mn, with a heterogeneous distribution of Mn concentration, generated a higher degradation rate of about 1.98 mm year^{-1} due to many micro-galvanic cells acting on the metal surface. This rate is higher than the one reported for the homogeneous Fe-Mn alloy [7].

The higher susceptibility of heterogeneous Fe-Mn alloys to corrosion could be ascribed to the presence of short-circuited galvanic cells acting on the surface of heterogeneous alloy. As the corrosion rate depends on the composition of the surrounding electrolyte, it should be tested in „in vivo“ conditions as to whether the corrosion rate of the above Fe-Mn alloy is sufficient for medical applications.

Acknowledgements

The authors are thankful for financial support of the research by the Slovak Research and Development Agency under contract APVV No. 0677-11 and VEGA grant 2/0168/12.

REFERENCES

[1] Yun, Y. et al.: Materials Today, vol. 12, 2009, p. 22
[2] Peuster, M., Hesse, C., Schloo, T., Fink, C., Beerbaum, P., von Schnakenburg, C: Biomaterials, vol. 27**,** 2006, p. 4955
[3] Waksman, R., Pakala, R., Baffour, R., Seabron, R., Hellinga, D., Tio, FO.: J. Interv. Cardiol, vol. 21, 2008, p. 15
[4] Peuster, M., Wohlsein, P., Brügmann,M., Ehlerding, M., Seidler, K., Fink, C., Brauer, H., Fischer, A., Hausdorf, G.: Heart, vol. 86, 2001, p. 563
[5] Hermawan, H., Dubé, D., Mantovani, D.: Acta Mater, vol. 6, 2009, p. 1693
[6] Hermawan, H., Dubé, D., Mantovani, D.: Journal of Biomedical Materials Research, Part A, vol. 93, 2010, no. 1, p. 1
[7] Hermawan, H., Purnama, A., Dube, D., Couet, J., Mantovani, D.: Acta Biomateria, vol. 6, 2010, p. 1852
[8] Moszner, F., Sologubenko, AS., Schinhammer, M., Lerchbacher, RC., Hänzi, AC., Leitner, H., Uggowitzer, PJ., Löffler, JF.: Acta Materialia, vol. 59, 2011, p. 981
[9] Schinhammer, M., Pecnik, CM., Rechberger, F., Hänzi, AC., Löffler, JF., Uggowitzer, PJ.: Acta Materialia, vol. 60, 2012, no. 6–7, p. 2746
[10] Hryha, E., Dudrová, E., Nyborg, L.: Metallurgical and Materials Transactions A : Physical Metallurgy and Materials Science, vol. 41, 2010, p. 2880